

# Mechanistic Understanding of Entanglement and Heralding in Cascade Emitters

K. Nasiri Avanaki<sup>†,‡</sup> and George C. Schatz<sup>\*,†</sup>

<sup>†</sup> *Department of Chemistry, Northwestern University, 2145 Sheridan Road, Evanston IL  
60208-3113, USA*

<sup>‡</sup> *Department of Chemistry and Chemical Biology, Harvard University, 12 Oxford Street,  
Cambridge MA 02138, USA*

E-mail: [g-schatz@northwestern.edu](mailto:g-schatz@northwestern.edu)

## Abstract

Semiconductor quantum light sources are favorable for a wide range of quantum photonic tasks, particularly quantum computing and quantum information processing. Here we theoretically investigate the properties of quantum emitters (QEs) as a source of entangled photons with practical quantum properties including heralding of on-demand single photons. Through the theoretical analysis, we characterize the properties of a cascade (biexciton) emitter, including (1) studies of single-photon purity, (2) investigating the first- and second- order correlation functions, and (3) determining the Schmidt number of the entangled photons. The analytical expression derived for the Schmidt number of the cascade emitters reveals a strong dependence on the ratio of decay rates of the first and second photons. Looking into the joint spectral density of the generated biphotons, we show how the purity and degree of entanglement are connected to the production of heralded single photons.

Our model is further developed to include polarization effects, fine structure splitting, and the emission delay between the exciton and biexciton emission. The extended model offers more details about the underlying mechanism of entangled photon production, and it provides additional degrees of freedom for manipulating the system and characterizing purity of the output photon. The theoretical investigations and the analysis provide a cornerstone for the experimental design and engineering of on-demand single photons.

**Keywords:** Cascade emission, Entangled photon, First and Second-correlation function, Schmidt number, Joint spectral density, Purity, Heralding, Polarization

Quantum light sources including on-demand single-photon sources are promising candidates in numerous frontier photonic and quantum technologies.<sup>1-4</sup> Embracing both experimental and theoretical investigations, single-photon emitters (SPE) as intrinsic building blocks play an essential role in quantum communication,<sup>5</sup> quantum computing<sup>4</sup> and quantum information processing.<sup>6</sup> In this area, a great deal of work has been done to characterize quantum light production using nonlinear crystals<sup>7</sup> or atomic systems,<sup>8</sup> both of which suffer from low photon emission rates and limited scalability. Moreover in a commonly used method of twin-state generation, spontaneous parametric down conversion,<sup>9,10</sup> the efficiency is low and depends on an inherently in-determinant emission processes.

Semiconductor quantum dots as non-classical light emitters are of particular interest and more favorable for single photon production<sup>11-14</sup> due to their high compatibility with the current semiconductor technology. It has been proven that these excellent quantum emitters<sup>11-15</sup> can produce single-photon states with high efficiency that are stimulated both by optical<sup>12</sup> and electrical<sup>16</sup> excitation. Moreover, recent advances in fabrication techniques have paved the road for the production of ideal semiconductor single-photon sources<sup>11,17-19</sup> showing that they possess significant capabilities for producing indistinguishable single-photons or entangled-photon pairs.<sup>17,20</sup> However the implementation depends upon the scalability of quantum emitters (QEs), so the on-demand generation of more complex photonic states is still a challenging task.

Generally, the characteristic properties of an ideal single-photon source can be classified into three categories: (i) single-photon purity in which the field does not accommodate more than one photon. This property is determined by the second-order intensity correlation function  $g^{(2)}(0)$  through the Hanbury Brown and Twiss (HBT) experiment.<sup>21,22</sup> (ii) indistinguishability, that is related to adjusting the quantum interference of two single-photon wavepackets and can be measured via Hong–Ou–Mandel (HOM) interference.<sup>23,24</sup> (iii) brightness in which one measures the probability that each light pulse contains a single photon. This measurement gives us more insight into the information contained in the second-order

coherence related to the photon number probabilities.<sup>22</sup>

These three properties have been defined differently depending on the scientific community, although the essential features behind them are the same: a single-photon source should generate light pulses with no more than one photon, the photon should be in a pure quantum state, and it should be generated as efficiently as feasible. All three of these essential features are determined by the second-order correlation function using different experiments.

In general correlation function measurements in the HBT experiment can be regarded as determining the probability of finding two or more photons in the same pulse. This is one of the parameters used to estimate the quality of the single photon source. This is significant on the grounds that high single-photon purity assures the security of quantum communications and minimizes errors in quantum computation and simulation.<sup>25,26</sup>

Bridging the concepts of an ideal SPE introduced here and the deficiency of scalable single-photon sources motivates the present work, in which we dig into the underlying mechanism for generation of close-to ideal twin-photon states. As part of this, we map out the characteristic parameters relevant to cascade entangled photon emission and show that single-photons derived from pairs generated by cascade emission can be prepared directly in pure states. In addition, we determine the degree of purity via correlation functions and we provide a Schmidt number analysis. Through these studies, we address major obstacles in the advancement of quantum photonics.

In our theoretical development, the generation of correlated photon pairs in semiconductor emitters is assumed to take place through a biexciton-exciton radiative cascade.<sup>11,13,14</sup> In this process, two electron-hole pairs form a biexciton state that radiatively decays with the emission of two photons as mediated by a single exciton state being an intermediate. The purity of the system is then limited by correlations within the photon pair as determined by the rates of decay of emission of the first and second photons.<sup>1,3,27</sup> This analysis is based on the fact that the radiative biexciton cascade in a single semiconductor QD provides a source of entangled photons.<sup>28,29</sup> Starting from the biexcitonic ground state of a pre-excited

QD, the first electron-hole recombination leads to emission of one photon, and then the second electron of opposite spin recombines with a hole to give a second photon with opposite polarization. This results in anticorrelation in the polarization of the emitted photons.<sup>30-33</sup>

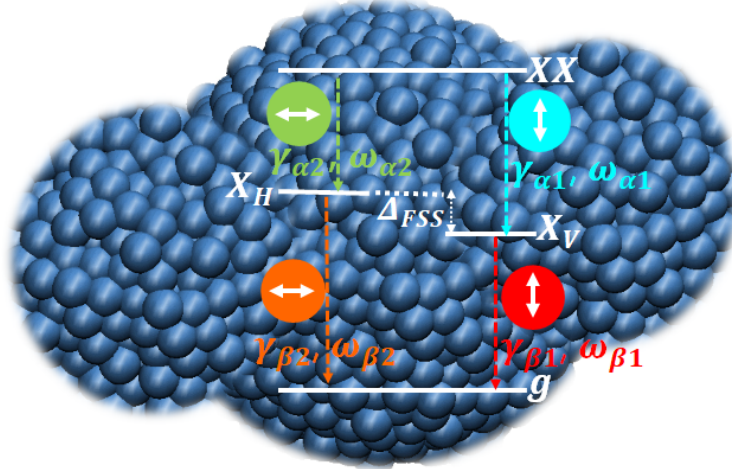


Figure 1: Schematic of radiative decay of the biexciton state  $|XX\rangle$  in a typical (asymmetric) QD with fine-structure splitting  $\Delta_{FSS}$ . Here we assume the radiative decay of  $|XX\rangle$  generates a pair of vertically or horizontally colinearly polarized photons;  $\frac{1}{\sqrt{2}}(|XX_HX_H\rangle + |XX_VX_V\rangle)$ .

Our analysis begins with the theoretical prediction just described, but then we progress to a more sophisticated cascade model that is needed when generating entangled photons from semiconductor QDs due to asymmetry in the geometry of the QDs. This imperfection induces splitting of the intermediate excitonic states, i.e., fine-structure splitting (FSS) ( $\Delta_{FSS}$ ), which is modified as QD size varies. This means that we are required to describe the QD biexciton cascade using a four-level system composed of the biexciton state ( $|XX\rangle$ ), two bright intermediate exciton levels ( $|X_{H(V)}\rangle$ ), and a ground state ( $|g\rangle$ ).<sup>34</sup> Spontaneous decay of the biexciton state to the ground state thus occurs via two intermediate exciton states leading to the emission of pairs of photons through the transitions  $|XX\rangle \rightarrow |X_{H(V)}\rangle$  and  $|X_{H(V)}\rangle \rightarrow |g\rangle$  respectively (see Fig. 1). Thus the intermediate excitonic states lead to spin-dependent properties of the emissions. With nonzero-FSS,<sup>35,36</sup> the degree of entanglement of the entangled polarization photon pairs is lower. However this can be modified

using promising strategies that have been proposed in previous studies.<sup>37–42</sup>

## Photon detection and quantum coherence functions in QEs

The essence of the HBT experiment is to recognize when the detectors are recording a photocurrent, since the detectors use the photoelectric effect to make local field measurements. For one detector, the photon counting rate is defined by a first-order correlation function,<sup>43</sup>  $G^{(1)}(\mathbf{r}, t) = \langle E^{(-)}(\mathbf{r}, t)E^{(+)}(\mathbf{r}, t) \rangle$ . Here the  $E^{(+/ -)}$ 's are positive and negative frequency parts of the fields and the detector is positioned at  $\mathbf{r}$ . For two photons and two detectors, the joint probability of observing one photoionization at point  $\mathbf{r}_2$  between  $t_2$  and  $t_2 + dt_2$  and another one at point  $\mathbf{r}_1$  between  $t_1$  and  $t_1 + dt_1$  with  $t_1 < t_2$  is governed by the second-order quantum mechanical correlation function which is measured in typical multi-photon counting experiments.

In the first part of this work we assume that we have a perfect symmetric QD that can produce highly entangled photons in which the FSS is zero (degenerate intermediate states). All spin and polarization properties are therefore hidden in the notation that we use to describe the states. In our cascade emission model, we define the almost perfectly symmetric excited QD as a three-level system where we use  $|e\rangle$  and  $|m\rangle$  instead of  $|XX\rangle$  and  $|X_{H(V)}\rangle$  for the excited and the intermediate states respectively. From Fig. 2, we assume that the system is initially ( $t = 0$ ) in the top level  $|e\rangle$  with energy  $\hbar(\omega_\alpha + \omega_\beta)$  and width  $\gamma_\alpha$ . This means that the lifetimes of the two-photon excited state is  $\gamma_\alpha^{-1}$ . The first spontaneous emission with frequency  $\omega_k$  is associated with the transition from  $|e\rangle$  to the intermediate state  $|m\rangle$  and the second decay is to the ground state  $|g\rangle$  via the emission of a photon of frequency  $\omega_q$ . It should be noted that when  $\gamma_\alpha > \gamma_\beta$ , there will be some population growth in the state  $|m\rangle$ , but if  $\gamma_\alpha \ll \gamma_\beta$ , the state  $|m\rangle$  lives for a short period of time and another photon is within a short time delay emitted in the second emission. The latter situation (slow emission followed by fast emission) is the circumstance that we mainly focus on in this

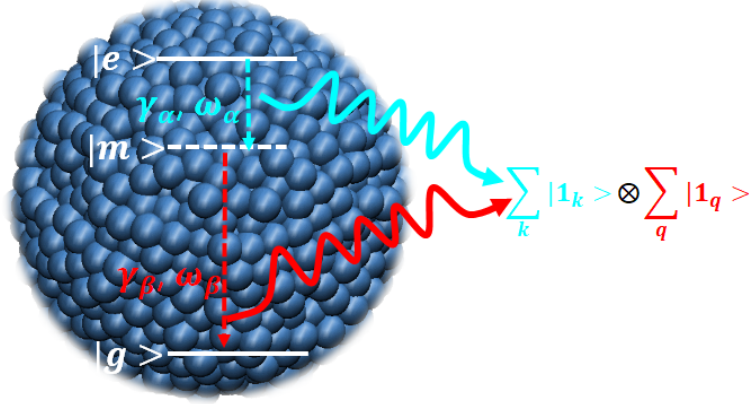


Figure 2: Symmetric (almost perfect) QD source: Three-level configuration used for observation of the two-photon cascade emission.

work.

## Power Spectrum Analysis: First-order Correlation Function

We assume that at time  $t = 0$  the emitter is in the excited state  $|e\rangle$  and the field modes are in the vacuum state  $|0\rangle$ . Given this, the state vector of the particle-field system at time  $t$  is described by

$$|\psi(t)\rangle = \eta_e(t) |e, 0\rangle + \sum_{\mathbf{k}} \eta_{m,\mathbf{k}}(t) |m, 1_{\mathbf{k}}\rangle + \sum_{\mathbf{k}\mathbf{q}} \eta_{g,\mathbf{k}\mathbf{q}}(t) |g, 1_{\mathbf{k}}, 1_{\mathbf{q}}\rangle \quad (1)$$

where the symbol  $|1_{\mathbf{k}}, 1_{\mathbf{q}}\rangle$  represents the tensor product  $|1_{\mathbf{k}}\rangle \otimes |1_{\mathbf{q}}\rangle$  of two single photon states of frequency  $\omega_{k(q)}$  of subsystem  $\alpha(\beta)$  with amplitude of  $\eta(\omega_{\mathbf{k}}, \omega_{\mathbf{q}}) \equiv \eta_{\mathbf{k}\mathbf{q}}$ . We determine the states of the particle and radiation field as a function of time using the Weisskopf-Wigner approximation where the particle in an excited state decays to the ground state with a characteristic lifetime but it does not make back and forth transitions. From the Schrödinger

equation we have

$$\left| \dot{\psi}(t) \right\rangle = -\frac{i}{\hbar} \widehat{H}_I |\psi(t)\rangle \quad (2)$$

Substituting Eq. 1 in the Schrödinger equation, we arrive at the equations of motion for the amplitudes  $\eta_e$ ,  $\eta_{m,k}$  and  $\eta_{g,k,q}$ ,

$$\begin{aligned} \dot{\eta}_e &= -i \sum_{\mathbf{k}} g_{\alpha\mathbf{k}} \eta_{m,\mathbf{k}} e^{i(\omega_\alpha - \omega_k)t} \\ \dot{\eta}_{m,\mathbf{k}} &= -i g_{\alpha\mathbf{k}} \eta_e e^{-i(\omega_\alpha - \omega_k)t} - i \sum_{\mathbf{q}} g_{\beta\mathbf{q}} \eta_{g,\mathbf{kq}} e^{i(\omega_\beta - \omega_q)t} \\ \dot{\eta}_{g,\mathbf{kq}} &= -i g_{\beta\mathbf{q}} \eta_{m,\mathbf{k}} e^{-i(\omega_\beta - \omega_q)t} \end{aligned} \quad (3)$$

We assume that the modes of the field are closely spaced in frequency, so we replace the summation over  $\mathbf{k}$  and  $\mathbf{q}$  by an integral,  $\sum_{\mathbf{k}} \rightarrow 2 \frac{V}{(2\pi)^3} \int_0^{2\pi} d\phi \int_0^\pi \sin\theta d\theta \int_0^\infty k^2 dk$ . Where  $V$  is the quantization volume. The transition dipole;  $e \langle i | \mathbf{r} | j \rangle = \boldsymbol{\mu}_{ij}$  and the radiative decay constants are then defined as

$$\begin{aligned} \gamma_\alpha &= \Gamma_\alpha/2 = \frac{1}{4\pi\epsilon_0} \frac{4\omega_\alpha^3 \mu_{em}^2}{3\hbar c^3} \\ \gamma_\beta &= \Gamma_\beta/2 = \frac{1}{4\pi\epsilon_0} \frac{4\omega_\beta^3 \mu_{mg}^2}{3\hbar c^3} \end{aligned} \quad (4)$$

Here  $g_{\alpha(\beta)}$  can be taken as a constant associated with the spontaneous emission rate.<sup>43</sup> We then carry out simple integration following Eq. 3,<sup>44</sup> and retrieve the probability amplitudes as

$$\begin{aligned} \eta_{m,\mathbf{k}}(t) &= -g_{\alpha,\mathbf{k}} \frac{e^{i(\omega_k - \omega_\alpha)t - \gamma_\alpha t} - e^{-\gamma_\beta t}}{(\omega_k - \omega_\alpha) + i(\gamma_\alpha - \gamma_\beta)} \\ \eta_{g,\mathbf{kq}}(t) &= \frac{g_{\alpha,\mathbf{k}} g_{\beta,\mathbf{q}}}{(\omega_k - \omega_\alpha) + i(\gamma_\alpha - \gamma_\beta)} \left\{ \frac{1 - e^{-\gamma_\beta t + i(\omega_q - \omega_\beta)t}}{\omega_q - \omega_\beta + i\gamma_\beta} - \frac{1 - e^{i(\omega_k + \omega_q - \omega_\alpha - \omega_\beta)t - \gamma_\alpha t}}{\omega_k + \omega_q - \omega_\alpha - \omega_\beta + i\gamma_\alpha} \right\} \end{aligned} \quad (5)$$

The first emission arises from the transition from  $|e\rangle$  to  $|m\rangle$ , at time  $t$ ,

$$-\sum_k g_\alpha \frac{\{e^{i(\omega_k - \omega_\alpha)t - \gamma_\alpha t} - e^{-\gamma_\beta t}\}}{(\omega_k - \omega_\alpha) + i(\gamma_\alpha - \gamma_\beta)} |m\rangle \otimes |1 : \omega_k, \alpha\rangle \quad (6)$$

This photon has a Lorentzian distribution in frequency with the width  $|\gamma_\alpha - \gamma_\beta|$ . If  $\gamma_\alpha \ll \gamma_\beta$ , then the state does not stay for a long time, the second photon is emitted soon such that the state is given by

$$\sum_{k,q} \frac{g_\alpha g_\beta}{(\omega_k - \omega_\alpha) + i(\gamma_\alpha - \gamma_\beta)} \left\{ \frac{1 - e^{-\gamma_\beta t + i(\omega_q - \omega_\beta)t}}{\omega_q - \omega_\beta + i\gamma_\beta} - \frac{1 - e^{i(\omega_k + \omega_q - \omega_\alpha - \omega_\beta)t - \gamma_\alpha t}}{\omega_k + \omega_q - \omega_\alpha - \omega_\beta + i\gamma_\alpha} \right\} |g\rangle \otimes |1_k, \alpha; 1_q, \beta\rangle \quad (7)$$

Defining  $\mathcal{N}_{EP}$  as the coefficient of the two-photon state ;  $\mathcal{N}_{EP} = g_\alpha g_\beta = \frac{2c\sqrt{\gamma_\alpha \gamma_\beta}}{V^{1/3}}$ , we may simplify the two-photon state in the long time limit (times long compared to the radiative decay,  $t \gg \gamma_\alpha^{-1}, \gamma_\beta^{-1}$ ):

$$|2P_{cas}\rangle = \sum_{kq} \eta_{\mathbf{k},\mathbf{q}}^{cas} |1_k, \alpha; 1_q, \beta\rangle \quad (8)$$

$$\eta_{\mathbf{k},\mathbf{q}}^{cas} = \frac{\mathcal{N}_{EP}}{(\omega_q - \omega_\beta + i\gamma_\beta)(\omega_k + \omega_q - \omega_\alpha - \omega_\beta + i\gamma_\alpha)}$$

It should be noted that in this limit, both  $\eta_{m,\mathbf{k}}(t)$  and  $\eta_e(t)$  are zero and only  $\eta_{\mathbf{k},\mathbf{q}}^{cas} \equiv \eta_{g,\mathbf{k},\mathbf{q}}(\infty)$  survives which is known as the "joint spectral amplitude".

In order to visualize the spectra of the emitted photons, here we look into the one-photon correlation function  $G^{(1)}(\tau)$ , and its normalized counterpart  $g^{(1)}(\tau)$ , which gives the degree of first-order temporal coherence between the emission fields at time  $t$  and  $t + \tau$  and takes the values  $0 \leq |g^{(1)}(\tau)| \leq 1$  for all light sources.<sup>43,45</sup>

$$G_m^{(1)}(\tau) = \langle E_m^{(-)}(t) E_m^{(+)}(t + \tau) \rangle$$

$$g_m^{(1)}(\tau) = \frac{\langle E_m^{(-)}(t) E_m^{(+)}(t + \tau) \rangle}{\langle E_m^{(-)}(t) E_m^{(+)}(t) \rangle} \quad m = \alpha, \beta \quad (9)$$

In the limit when the line width ( $\gamma_{\alpha(\beta)}$ ) goes to zero, the light field is perfectly coherent and  $g^{(1)}(\infty) = 1$ . Using the above expression, the first-order correlation for a linear polarized field  $E^{(+)}(\mathbf{r}, t) = \sum_k \hat{a}_{\mathbf{k}} e^{-i\omega_k t + i\mathbf{k} \cdot \mathbf{r}}$  is obtained as;

$$G_{\alpha}^{(1)}(\tau) = e^{i\omega_{\alpha}\tau - (\gamma_{\alpha} + \gamma_{\beta})|\tau|}, \quad G_{\beta}^{(1)}(\tau) = e^{i\omega_{\beta}\tau - \gamma_{\beta}|\tau|} \quad (10)$$

However, an important property of the first-order correlation function is that it forms a Fourier transform pair with the power spectrum expressed as:  $S(\omega) = \frac{1}{\pi} \text{Re} \int_0^{\infty} d\tau G^{(1)}(\tau) e^{-i\omega\tau}$ . The spectrum is obtained by performing a photon number measurement for a specific mode on a given state, i.e. for a given two-photon state density  $\rho$ , its spectrum is given by  $S(\omega) = \text{Tr}[\hat{a}^{\dagger}(\omega)\hat{a}(\omega)\rho]$ . Using Eq. 5, we arrive at

$$\begin{aligned} G_{\alpha}^{(1)}(\omega) &= \sum_k |\eta_m(\omega, \omega_k)|^2 \\ G_{\beta}^{(1)}(\omega) &= \sum_k |\eta_g(\omega_k, \omega)|^2 \end{aligned} \quad (11)$$

Hence, the distribution of the emitted photons in the frequency domain is the power spectrum, expressed as

$$\begin{aligned} S_{\alpha}(\omega) &= \frac{2c}{V^{1/3}} \frac{\gamma_{\alpha} + \gamma_{\beta}}{(\omega - \omega_{\alpha})^2 + (\gamma_{\alpha} + \gamma_{\beta})^2} \\ S_{\beta}(\omega) &= \frac{2c}{V^{1/3}} \frac{\gamma_{\beta}}{(\omega - \omega_{\beta})^2 + \gamma_{\beta}^2} \end{aligned} \quad (12)$$

We see that the distribution  $S_{\alpha}(\omega)$  associated with the first photon is given by a Lorentzian centered at  $\omega_{\alpha}$  and the width at half-maximum is the sum of the natural widths;  $2(\gamma_{\alpha} + \gamma_{\beta})$ . In the same fashion, the power spectrum of the second photon is given by  $S_{\beta}(\omega)$ , leading to a Lorentzian curve of width at half-maximum  $2\gamma_{\beta}$ , localized around  $\omega_{\beta}$ . These bandwidths are measures of the coherence time of the emissions.

Note that for a general pure two-photon state  $|2P_{cas}\rangle = \sum_{kq} \eta(\omega_k, \omega_q) |1 : \omega_k, \alpha; 1 : \omega_q, \beta\rangle$ ,

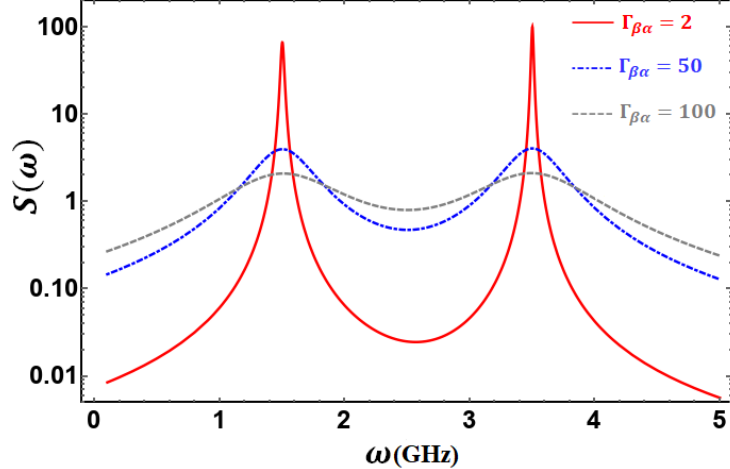


Figure 3: Total spectral density in cascade fluorescence (Eq. 13). In these set of calculations we assume that  $\gamma_\alpha = 0.005$  GHz,  $\omega_\alpha = 1.5$  GHz and  $\omega_\beta = 3.5$  GHz, as described in the text. Different colors show how the spectra and density change as the ratio of  $\Gamma_{\beta\alpha} = \frac{\gamma_\beta}{\gamma_\alpha}$  varies.

we define the spectral density based on summing up the lineshapes of the photons:  $S_{2EP}(\omega) = \sum_k |\eta(\omega_k, \omega)|^2 + |\eta(\omega, \omega_k)|^2$ . This means, the emitted photon power spectrum is only determined by the diagonal elements of the corresponding density matrix. This also indicates that the spectrum of a pure two-photon state is the same as that from the corresponding diagonal density matrix.

Therefore the total spectral density is a blend of two Lorentzian functions with central frequencies  $\omega_\alpha$ ,  $\omega_\beta$  and widths  $\gamma_\alpha + \gamma_\beta$  and  $\gamma_\beta$  respectively.

$$S_{2EP}(\omega) = \frac{2c}{V^{1/3}} \left[ \frac{\gamma_\alpha + \gamma_\beta}{(\omega - \omega_\alpha)^2 + (\gamma_\beta + \gamma_\alpha)^2} + \frac{\gamma_\beta}{(\omega - \omega_\beta)^2 + \gamma_\beta^2} \right] \quad (13)$$

In Fig. 3, we plot the spectral density for cascade fluorescence (right panel). Different colors show how the spectra change as the ratio of  $\gamma_\beta/\gamma_\alpha$  varies. The structure of the emission spectrum and the tail behavior of the density is in agreement with a previous work.<sup>46</sup> The bimodal shape of the spectrum originates from overlap of the two emissions as can be explained based on the contribution of each state according to its density of states. In this figure, and elsewhere in this paper, we performed our calculations using parameters in

the same range as polarization-entangled photon pairs from a biexciton cascade from a single InAs QD embedded in a GaAs/AlAs planar microcavity.<sup>37,47</sup> In those experiments the pair of entangled photon emissions are at 1.398 eV and 1.42 eV. The following references<sup>30,48–50</sup> are also relevant.

## Second-order Correlation Function

Now consider the HBT experiment with a multiphoton source, where we look for the rate of coincidences in the photon-count rates using two detectors. This rate is governed by a second-order correlation function defined as,

$$G^{(2)}(\mathbf{r}, \mathbf{r}', t, t') = \langle \psi | E^{(-)}(\mathbf{r}, t) E^{(-)}(\mathbf{r}', t') E^{(+)}(\mathbf{r}', t') E^{(+)}(\mathbf{r}, t) | \psi \rangle \quad (14)$$

in which the normalized form is

$$g^{(2)}(\mathbf{r}, \mathbf{r}', t, t') = \frac{\langle E^{(-)}(\mathbf{r}, t) E^{(-)}(\mathbf{r}', t') E^{(+)}(\mathbf{r}', t') E^{(+)}(\mathbf{r}, t) \rangle}{\langle E^{(-)}(\mathbf{r}, t) E^{(+)}(\mathbf{r}, t) \rangle \langle E^{(-)}(\mathbf{r}', t') E^{(+)}(\mathbf{r}', t') \rangle} \quad (15)$$

Here  $|\psi\rangle = \sum_{\mathbf{k}\mathbf{q}} |1_{\mathbf{k}}, 1_{\mathbf{q}}\rangle$  is the two photon state, and the correlation function refers to detection of photon  $\mathbf{k}$  (at  $\mathbf{r}, t$ ) followed by detection of photon  $\mathbf{q}$  (at  $\mathbf{r}', t'$ ).

In this work, the second-order correlation function for two-photon emission from cascade emitters can be recast as

$$\begin{aligned} G^{(2)}(t, t') &= \langle 2P_{cas} | E_{\alpha}^{(-)}(t) E_{\beta}^{(-)}(t') E_{\beta}^{(+)}(t') E_{\alpha}^{(+)}(t) | 2P_{cas} \rangle \\ &= \sum_{\{n\}} \langle 2P_{cas} | E_{\alpha}^{(-)}(t) E_{\beta}^{(-)}(t') | \{n\} \rangle \langle \{n\} | E_{\beta}^{(+)}(t') E_{\alpha}^{(+)}(t) | 2P_{cas} \rangle \\ &= \langle 2P_{cas} | E_{\alpha}^{(-)}(t) E_{\beta}^{(-)}(t') | 0 \rangle \langle 0 | E_{\beta}^{(+)}(t') E_{\alpha}^{(+)}(t) | 2P_{cas} \rangle \\ &= \Psi^{*(2)}(t, t') \Psi^{(2)}(t, t') \end{aligned} \quad (16)$$

Where we defined  $\Psi^{(2)}(t, t') \equiv \langle 0 | E_{\alpha}^{(+)}(t) E_{\beta}^{(+)}(t') | 2P_{cas} \rangle$ . Note here that a complete set of

states;  $(\sum_{\{n\}} |\{n\}\rangle \langle\{n\}| = 1)$  is included. Since our two-photon state consists of  $|1_k, 1_q\rangle$  and is annihilated by  $E^{(+)}(t)E^{(+)}(t')$ , only the  $|0\rangle \langle 0|$  term survives, making the final form of Eq. 16 relatively simple. (It is also true that only the vacuum level persists at long times in the complete wavefunction).

Making use of the two-photon state introduced earlier in Eq. 8 for the detection at times  $t$  and  $t + \tau$ , we then arrive at<sup>43</sup>

$$\begin{aligned} \Psi^{(2)}(t, t + \tau) &\equiv \langle 0 | E_{\alpha}^{(+)}(t) E_{\beta}^{(+)}(t + \tau) | 2P_{cas} \rangle \\ &= \sum_{kq} \eta_{cas} e^{-i\omega_k t - i\omega_q(t+\tau)} \\ &= -\frac{V^{1/3}}{c} \sqrt{\gamma_{\alpha} \gamma_{\beta}} e^{-(i\omega_{\alpha} + i\omega_{\beta} + \gamma_{\alpha})t} \Theta(t) e^{-(i\omega_{\beta} + \gamma_{\beta})\tau} \Theta(\tau) \end{aligned} \quad (17)$$

Here  $\Theta(t)$  is a unit step function. If we are considering the HBT experimental setup with two detectors ( $D_1$  and  $D_2$ ) for the measurements, the first term in the above expression indicates that the  $\omega_{\alpha}$  photon goes to the  $D_1$  detector and the second photon  $\omega_{\beta}$  to  $D_2$ . This amplitude should be added to the vice-versa situation to determine the total amplitude, where the latter has the same form here since both detectors are assumed to be located the same distance from the QD source. Substituting the final expression from Eq. 17 into Eq. 16 and ultimately back into Eq. 15, we see in our bipartite system, the correlations between parts can be determined with the help of the following (normalized) cross temporal correlation function,

$$\begin{aligned} g_{\times}^{(2)}(t, t + \tau) &= \frac{\langle 2P_{cas} | E_{\alpha}^{(-)}(t) E_{\beta}^{(-)}(t + \tau) E_{\beta}^{(+)}(t + \tau) E_{\alpha}^{(+)}(t) | 2P_{cas} \rangle}{\langle 2P_{cas} | E_{\alpha}^{(-)}(t) E_{\alpha}^{(+)}(t) | 2P_{cas} \rangle \langle 2P_{cas} | E_{\beta}^{(-)}(t + \tau) E_{\beta}^{(+)}(t + \tau) | 2P_{cas} \rangle} \\ &\approx \frac{V^{2/3}}{c^2} \frac{\gamma_{\alpha} \gamma_{\beta}}{\pi^2} \left( \frac{\gamma_{\beta}}{\gamma_{\alpha}} - 1 \right) \left[ \Theta(t) e^{-2\gamma_{\alpha} t} \Theta(\tau) e^{-2\gamma_{\beta} \tau} + \Theta(-\tau) e^{2(\gamma_{\beta} - \gamma_{\alpha})\tau} \Theta(t + \tau) e^{-2\gamma_{\alpha} t} \right] \end{aligned} \quad (18)$$

With regards to the use of entangled photons in quantum photonics, there are always some concerns about pure and reproducible entangled photon generation if the QD is degraded or if the QD is re-excited after the entangled photons are emitted or background photons

are present. Therefore the purity of the single-photon source is critical for high fidelity QD-photon entanglement, and this generally can be evaluated through the HBT setup, where the following experimentally relevant cross-correlation function is measured,

$$g_{\times}^{(2)}(\tau) = \langle g_{\times}^{(2)}(t, t + \tau) \rangle_t = \lim_{T \rightarrow \infty} \int_{-T}^T g_{\times}^{(2)}(t, t + \tau) dt \quad (19)$$

Here the total detection time  $T$  is taken to be long compared to the single photon pulsewidth ( $T \rightarrow \infty$ ). The above formulation involves calculating the normalized time dependent second-order correlation function after integrating for a long enough time,  $\langle g_{\times}^{(2)}(t, t + \tau) \rangle_t$ .<sup>51</sup> The purity of the system as a single-photon source is then extracted from  $g_{\times}^{(2)}(\tau = 0)$ .<sup>52-54</sup> For our three-level model of Cascade emission the second-order correlation function is found to be

$$g_{\times}^{(2)}(\tau) \approx \frac{V^{1/3}}{c} \frac{\gamma_{\beta}}{\pi} \left( \frac{\gamma_{\beta}}{\gamma_{\alpha}} - 1 \right) \left[ \Theta(\tau) e^{-2\gamma_{\beta}\tau} + \Theta(-\tau) e^{2\gamma_{\beta}\tau} \right] \quad (20)$$

Here we see that  $g_{\times}^{(2)}(\tau)$  decays exponentially with  $|\tau|$ , which makes sense given that the second photon is emitted very shortly after the first. Also,  $g_{\times}^{(2)}(\tau = 0)$  depends on the radiative decay rates of the two emissions, which is in agreement with the previous studies<sup>51,55,56</sup>, and the quantization volume also plays a role.<sup>51</sup> When  $\gamma_{\alpha} \ll \gamma_{\beta}$ ,  $g_{\times}^{(2)}(0) > 0$ , and a positive pure cross correlation is found. Generally, the area of the peak;  $g_{\times}^{(2)}(\tau)$  around  $\tau \sim 0$  (0th peak) gives the normalized coincidence detection probability when two photons are incident in different inputs of the beam splitter in the HBT experimental setup. Only in the limit  $\gamma_{\alpha} = \gamma_{\beta}$  does this area go to zero. This makes sense as in this limit there is no entanglement (see later discussion of Schmidt numbers).

In this derivation, we have assumed that a light pulse interacts with the system to produce the initial biexciton excited state, and then this decays with no correlation to its initial preparation. However in the actual experimental setup a series of pulses is typically used to excite the system, and there may exist some amplitude from a previous pulse that has

not decayed to zero when the next pulse arrives. This leads to a series of peaks in the  $g_{\times}^{(2)}(\tau)$  function, but this is not important in the present study. We also note that the inclusion of coherence between the excitation and emission steps will lead to a more complex peak at  $\tau = 0$ , as has often been discussed for other emitters.<sup>52–54,57</sup> As we did in the time domain, in

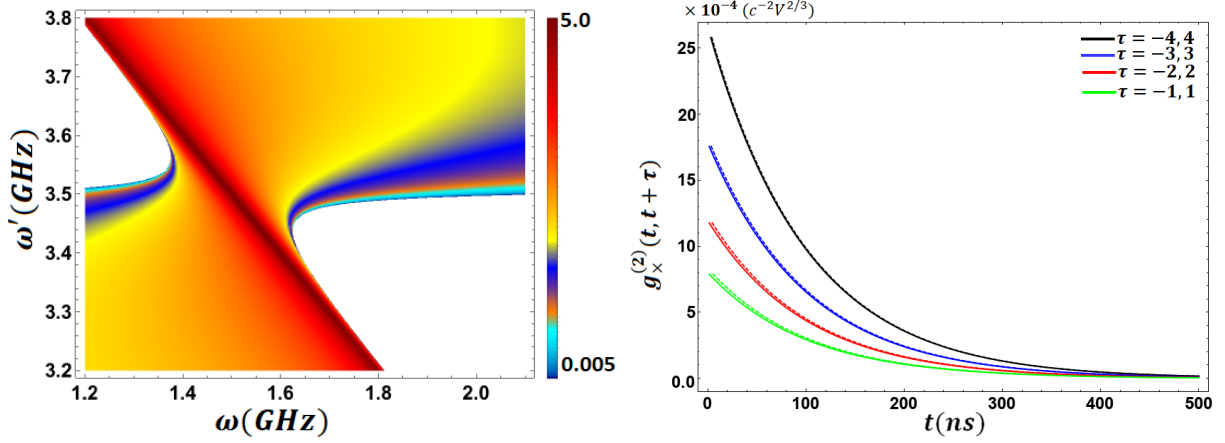


Figure 4: Left: Second-order frequency cross correlation function  $g_{\times}^{(2)}(\omega, \omega')$  for the cascade emission process in the frequency domain (logarithmic scale). Right:  $g_{\times}^{(2)}(t, t + \tau)$ , the normalized cross temporal correlation function. Here  $\gamma_{\beta}/\gamma_{\alpha} = 40$ ,  $\gamma_{\alpha} = 0.005$  GHz,  $\omega_{\alpha} = 1.5$  GHz and  $\omega_{\beta} = 3.5$  GHz.

order to fully describe the correlations between two emissions, at different frequencies,  $\omega$  and  $\omega'$ , one would have to compute a double Fourier transform according to the cross-correlation definition;  $g_{\times}^{(2)}(\omega, \omega') = \frac{1}{\pi^2} \text{Re} \int_{-\infty}^{\infty} \int_{-\infty}^{\infty} dt dt' e^{-i\omega t} e^{-i\omega' t'} g_{\times}^{(2)}(t, t')$ . This function provides a measure of resemblance of the two photons as a function of the frequency displacement of one relative to the other. Applying the cross-correlation definition to Eq. 18, we obtain:

$$g_{\times}^{(2)}(\omega, \omega') \approx \frac{\gamma_{\alpha}\gamma_{\beta}}{\pi^2} \left(\frac{\gamma_{\beta}}{\gamma_{\alpha}} - 1\right) \frac{4\gamma_{\alpha}\gamma_{\beta} + (\omega + \omega' - \omega_{\alpha} - \omega_{\beta})(\omega' - \omega_{\beta})}{[(\omega + \omega' - \omega_{\alpha} - \omega_{\beta})^2 + 4\gamma_{\alpha}^2][(\omega' - \omega_{\beta})^2 + 4\gamma_{\beta}^2]} \quad (21)$$

This function is useful as it determines the width of the frequency anticorrelation associated with the two emitted photons.

In Fig. (4), the  $g_{\times}^{(2)}$  function in both time (right) and frequency (left) domains is depicted. In the left plot, one observes that the function has significant values only on the anti-diagonal, along the line  $\omega + \omega' = \omega_{\alpha} + \omega_{\beta}$ . This implies that the corresponding states exhibit strong

frequency anticorrelation. The width of the anti-diagonal which gives the characteristic width of the frequency anticorrelation, is equal to  $\gamma_\alpha$ . In the right panel of Fig. (4),  $g_\times^{(2)}$  from Eq. 18 is plotted versus  $t$  for different values of time delay  $\tau$  and with  $\gamma_\alpha < \gamma_\beta$ . The illustration shows the expected exponential decay of  $g_\times^{(2)}$  with  $t$  as determined by the  $\gamma_\alpha$  rate, and also that there is exponential decay as a function of  $\tau$  as determined by  $\gamma_\beta$ . Note that negative anti-correlation is obtained when  $\gamma_\alpha > \gamma_\beta$ , which is consistent with the recent study.<sup>55</sup>

## Heralded Single Photons

So far we have studied the properties of emitted entangled photons and the role of the relevant spectral parameters in the emission spectrum. In this section, we focus on the influence of frequency correlation on the purity of heralded single photons that are derived from the two photon state. In the frequency dependence of the general state from a cascade emitter, the two-photon component can be obtained from Eq. 8 which represents a pure state. Here the joint spectral amplitude generally contains correlations between frequencies of the sibling photons. As a result of this combination of purity and correlation,  $|2P_{cas}\rangle$  is entangled in the frequency of the two product photons. The purity of either heralded single photon that originates from  $|2P_{cas}\rangle$  can then be determined from the density matrix. It is worth recalling that, this property is *inversely* related to the degree of the entanglement of our two-photon state. For a bipartite two-photon source, the density matrix (from Eq. 8) reads as

$$\rho^{cas} = |2P_{cas}\rangle \langle 2P_{cas}| = \sum_{\mathbf{k}\mathbf{q}} |\eta_{\mathbf{k},\mathbf{q}}^{cas}|^2 |1_{\mathbf{k}}, \alpha; 1_{\mathbf{q}}, \beta\rangle \langle 1_{\mathbf{k}}, \alpha; 1_{\mathbf{q}}, \beta| \quad (22)$$

where  $|\eta_{\mathbf{k},\mathbf{q}}^{cas}|^2$  is the joint spectral probability density. The purity of either heralded single photon derived from  $|2P_{cas}\rangle$  is related to the two reduced density operators of the partner

photons, given by:

$$\begin{aligned}\rho_\alpha &= \text{Tr}_\beta \rho = \sum_k \xi_k |1 : \omega_k, \alpha\rangle \langle 1 : \omega_k, \alpha|, & \text{where } \xi_k &= \sum_q \eta_{kq} \\ \rho_\beta &= \text{Tr}_\alpha \rho = \sum_q \zeta_q |1 : \omega_q, \beta\rangle \langle 1 : \omega_q, \beta|, & \text{where } \zeta_q &= \sum_k \eta_{kq}.\end{aligned}\tag{23}$$

The purity of the individual photons is then determined using

$$\mathcal{P}_\alpha = \text{Tr}(\rho_\alpha^2), \quad \mathcal{P}_\beta = \text{Tr}(\rho_\beta^2).\tag{24}$$

To see how the spectral correlations in  $|2P_{cas}\rangle$  are involved in the purity of the heralded single photons, we examine the Schmidt decomposition of the joint two-photon state. Schmidt decomposition is a characteristic method for describing a bipartite system in terms of a complete set of basis states. Through this decomposition, one can calculate the Schmidt number which defines the ‘‘degree’’ of entanglement of the two-photon state. In this decomposition, Eq. 8 becomes<sup>58–60</sup>

$$|2P_{cas}\rangle = \sum_k \sqrt{\lambda_k} |\phi_k^\alpha\rangle \otimes |\phi_k^\beta\rangle, \quad \text{where } \langle \phi_k^\mu | \phi_q^\mu \rangle = \delta_{kq}, \quad \text{and } \sum_k \lambda_k = 1.\tag{25}$$

The orthonormal basis states  $|\phi_{k(q)}^\mu\rangle$  ( $\mu = \alpha, \beta$ ) are known as Schmidt modes which can be thought of as the basic building blocks of entanglement in the sense that if the first photon is described by a function  $|\phi_k^\alpha\rangle$ , we know with certainty that its second sibling is determined by the corresponding function  $|\phi_k^\beta\rangle$ . Note that each set depends only on one subsystem of  $|2P_{cas}\rangle$  and each pair of modes is weighted by its Schmidt magnitude,  $\lambda_k$ . The number of mandatory non-zero components in the sum needed to construct the  $|2P_{cas}\rangle$  state (in terms of its Schmidt modes), indicates the effective number of modes that are correlated, while the homogeneity in the distribution of coefficients is determined by the Schmidt number,  $\kappa$ ,

expressed as

$$\kappa = \frac{1}{\text{Tr}(\rho_\alpha^2)} = \frac{1}{\text{Tr}(\rho_\beta^2)} = \frac{1}{\sum_{k=1}^N \lambda_k^2} \quad (26)$$

Comparing Eq. 26 and Eq. 24, we realize that the purity of both reduced states is equal to the sum of the squares of the Schmidt coefficients and thus the inverse of the Schmidt number;  $\mathcal{P}_{\alpha(\beta)} = 1/\kappa$ . From the experimental point of view, this is relevant to the expected number of required modes. It should also be pointed out that the number of non-zero Schmidt coefficients in the sum is called the Schmidt rank, or sometimes the dimensionality of the entanglement, as it represents the minimum local Hilbert space dimension required to correctly represent correlations of the quantum state.<sup>60</sup>

## Schmidt Analysis

We now provide an analytical determination of the Schmidt number for the cascade emitter. Different numerical and analytical frameworks for the Schmidt decomposition of paired photons have been proposed<sup>58-61</sup> which we can use to advantage for characterizing separability/purity of our bipartite two-photon state. To describe the cascade emission presented by  $|2P_{cas}, \alpha\beta\rangle = \sum_{k,q} \eta(\omega_k, \omega_q) |1 : \omega_k, \alpha; 1 : \omega_q, \beta\rangle$ , we introduce  $|\psi_k\rangle \propto \sum_m \eta(\omega_m, \omega_k) |1 : \omega_m\rangle$  as a basis set in which we should find the normalization factor first ( i.e.  $\langle\psi_j|\psi_k\rangle = \sum_m \eta(\omega_m, \omega_k)\eta^*(\omega_m, \omega_j)$ ). We then construct the reduced density matrix. In our mathematical approach, we approximate the normalized  $|\psi_k\rangle$  as a piece-wise state  $|\phi_s\rangle$  by discretizing  $\omega_k$  into a small interval of  $2\gamma_\alpha$ , i.e.  $\omega_k = 2N_s\gamma_\alpha$  where  $N_s$  is an integer. The normalized basis set is therefore defined as

$$|\phi_s\rangle \approx \sqrt{\frac{\pi}{\gamma_\beta} \frac{(2\gamma_\alpha N_s - \omega_\beta)^2 + \gamma_\beta^2}{4\gamma_\alpha^2}} \int_{2\gamma_\alpha N_s}^{2\gamma_\alpha(N_s+1)} \sum_m \eta(\omega_m, \omega) d\omega |1 : \omega_m\rangle \quad N_s = \omega_k/2\gamma_\alpha \quad (27)$$

Here we have approximated the sum over 'm' as  $\sum_m \leftrightarrow \int \frac{L}{2\pi c} d\omega_m$  and used Cauchy's integral theorem. Then the orthonormal relations read as  $\langle \phi_r | \phi_s \rangle \approx \delta_{rs}$  and we obtain the reduced density matrix within a very good approximation as (see more details in SI).

$$\rho^{red} = \sum_{N_s} \frac{\gamma_\beta}{\pi} \frac{2\gamma_\alpha}{(2\gamma_\alpha N_s - \omega_\beta)^2 + \gamma_\beta^2} |\phi_s\rangle \langle \phi_s| \quad (28)$$

Accordingly the ‘‘Schmidt coefficients’’  $\{\sqrt{\lambda_s}\}$  are given by the square roots of the eigenvalues of the reduced density matrix,  $\sqrt{\lambda_s} \approx \sqrt{\frac{\gamma_\beta}{\pi} \frac{2\gamma_\alpha}{(2\gamma_\alpha N_s - \omega_\beta)^2 + \gamma_\beta^2}}$  and we can simply show that  $\sum_s \lambda_s \approx 1$ .

Generally finding an analytical expression for Schmidt modes and Schmidt number is tricky and complicated. However using the purity definition which is the inverse of the Schmidt number, it is possible to obtain the Schmidt number with no further approximation. Thus the Schmidt number of the bipartite two photon state generated by cascade emission can be obtained from Eq. 26. The resulting formula after some lengthy algebra is:

$$\kappa = \frac{1}{\sum_{mn} |\sum_k \eta_{km} \eta_{kn}^*|^2} = 1 + \frac{\gamma_\beta}{\gamma_\alpha} \quad (29)$$

We see that the minimum Schmidt number from this analysis falls at unity corresponding to the limit  $\gamma_\alpha \gg \gamma_\beta$ . For this situation, the population of the doubly excited state in the three-level QD source will decay to the intermediate state within a very short time, and then the transition from intermediate level to ground state occurs on a longer time scale. Therefore, the total energy of the two-photon state varies significantly as a function of time, and there is weak frequency anti-correlation. Also, if  $\gamma_\alpha$  is extremely large, de-excitation from the top state occurs instantaneously after coupling to the radiation field is turned on, and the second photon is uncorrelated from the first.

If  $\gamma_\alpha$  is very small compared with  $\gamma_\beta$ , then the second photon is emitted soon after the first photon emission, and the fluctuations in the total energy of the two-photon state will be negligible. This implies that the two photons have strong frequency anti-correlation, which is

consistent with our earlier analysis. In the extreme case where  $\gamma_\alpha$  is close to zero, the photon pairs are fully frequency-anticorrelated, the expression for  $\eta_{kq}$  breaks down into  $\eta(\omega_k, \omega - \omega_k)$ , and the state is clearly in the form of a Schmidt decomposition. Due to the flatness of the

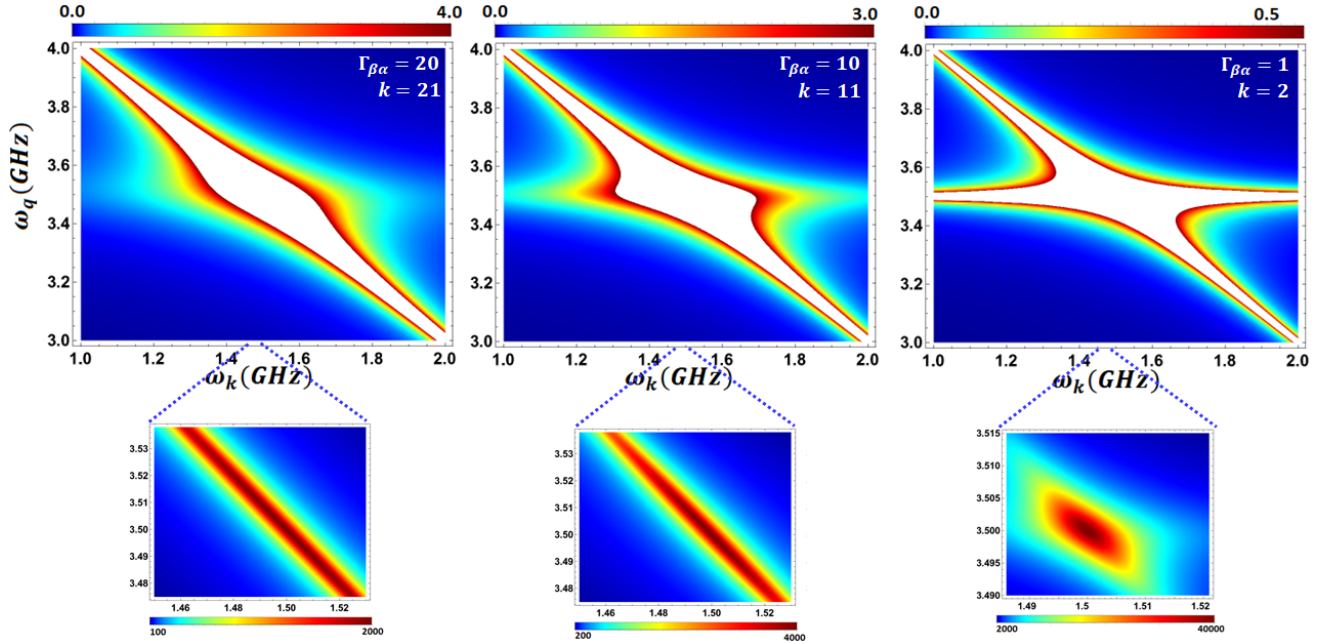


Figure 5: Joint spectral density (JSD) of QD emitter in three-level model. JSD profile goes from a broad linewidth ( $\gamma_\alpha$ ) to being symmetric along the diagonal while the ratio of  $\Gamma_{\beta\alpha} = \gamma_\beta/\gamma_\alpha$  is increased. Here we assume that  $\gamma_\alpha = 0.005$  GHz,  $\omega_\alpha = 1.5$  GHz and  $\omega_\beta = 3.5$  GHz.

distribution of Schmidt coefficients, the corresponding Schmidt number can be very large. From this we conclude that a larger ratio of  $\gamma_\beta/\gamma_\alpha$  gives rise to better frequency correlations i.e. stronger entanglement of the total state.

In contrast to the high entanglement case, to collect heralded single photons in a pure state, one must ensure that the relevant parameters of the system closely meet the condition;  $\gamma_\alpha \gg \gamma_\beta$ . This also means that to separate the entangled photons into two single photons, one should reduce correlations such that the Schmidt number has a low value. For the cascade source we consider, the only way this can be done is to make the joint spectral density given by  $|\eta_{\mathbf{k},\mathbf{q}}^{cas}|^2$  be factorable.

We plot the Joint Spectral Density (JSD) in Fig. 5. This characterizes the joint spectrum

of the two photons, and it can be manipulated via the emission bandwidths and by other relevant parameters of the two photon state. Experimentally this can be done by measuring the JSD profile with tunable narrow band filters<sup>62</sup> in a same manner as HOM quantum interference quantifies the two-photon coherence bandwidth and the indistinguishability of the photon pair. This is a common method for heralding the signal and idler photons in a parametric down conversion experiment.

The JSDs in Fig. 5 illustrate how the frequency correlation is related to the degree of entanglement of states of the two-photons when the ratio of  $\gamma_\beta/\gamma_\alpha$  is changed. Here the vertical and horizontal axes show the frequencies of the first and second emissions. The direct consequences of the entanglement are seen when the Schmidt number is decreased (going from the left to the right) over the range  $\kappa = 21 - 2$ . The results indicate that the probability of frequency correlation is highest in a very short range close to the transition frequencies,  $\omega_\alpha$  and  $\omega_\beta$ . Noticeably we see that the distribution is highly aligned with the anti-diagonal wherein  $\omega_\alpha + \omega_\beta = \omega_k + \omega_q$  when  $\kappa$  is high. As  $\kappa$  is decreased there is a broadening of the distribution centered on  $\omega_q = \omega_\beta$ . Also, the correlation intensity is reduced as the JSD profile goes from being closely aligned along the anti-diagonal to a broadened line shape. We may conclude that the more asymmetric and spread-out is the spectral density, the less entangled the photons are.

The images in figure Fig. 5 also zoom in for a smaller frequency range around the anti-diagonal, and paying closer attention to the middle part of these distributions in which the intensity is very high. Overall, we recognize that a biphoton state can be ideally suited for generating heralded pure-state single photons when the side lobes that hinder the generation of the entangled photon, symmetrically are enhanced. Although the JSD is very informative about the properties of the states, the JSD alone is insufficient to conclude that they are frequency entangled.<sup>60</sup>

# Polarization Effects in Entangled Photons

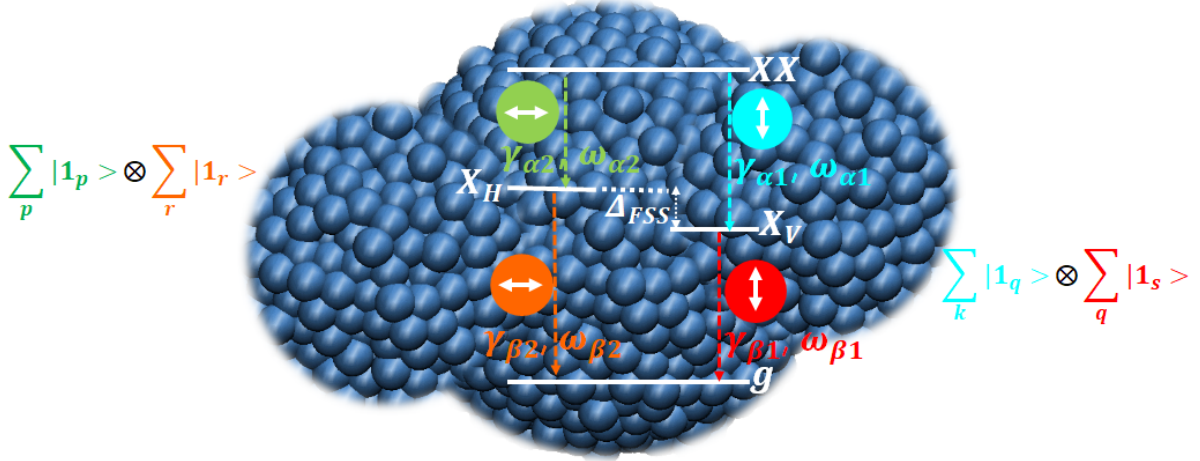


Figure 6: Entangled photon generation from biexciton cascade emission: The final two-photon state is created by sequential emission of two photons (XX and X) separated by a short time delay  $\tau$ . The resulting state is a superposition of horizontal (H) and vertical (V) polarization states.

As we explained in the introduction section, it is more appropriate if we define a QD biexciton cascade using a four-level system composed of a biexciton state (XX), two bright intermediate exciton levels ( $X_{H(V)}$ ) with different polarizations (either horizontal (H) or vertical (V)) and a ground state (g). Therefore, the decay proceeds via one of two paths (See Fig. 6). Here we assume that the system is initially in a superposition of the biexciton-exciton photonic states. After emitting the first photon, it evolves to the exciton (X) state in which the degeneracy is split. The quantum dot remains in a superposition of  $X_H$  and  $X_V$  for a time delay  $\tau_e$ , during which a phase difference develops due to the fine structure splitting  $\Delta_{\text{FSS}}$  between different exciton states. Finally, the exciton photon  $X_{H(V)}$  with the same polarization as the first biexciton photon is emitted, and the QD goes back to the ground state. The system is now found in a superposition of orthogonally polarized photon pair states, with a phase between them that is characterized by the time delay  $\tau_e$  (generally in the order of tens of ps). If we denote the state of the photon in each emission by the corresponding state of the QD, including for the polarization effect, our cascade two-photon

emission wavefunction in Eq. 8 is modified to:

$$\begin{aligned}
|2P_{cas}\rangle &= \frac{1}{\sqrt{2}} \left( \sum_{p,r} \eta_{p,r}^{(H)} |XX_H X_H\rangle + \sum_{q,s} \eta_{q,s}^{(V)} |XX_V X_V\rangle \right) \quad \text{for } \Delta_{\text{FSS}} = 0 \\
|2P_{cas}\rangle &= \frac{1}{\sqrt{2}} \left( \sum_{p,r} \eta_{p,r}^{(H)} |XX_H X_H\rangle + \sum_{q,s} \eta_{q,s}^{(V)} e^{i\Delta_{\text{FSS}}\tau_e/\hbar} |XX_V X_V\rangle \right) \quad \text{for } \Delta_{\text{FSS}} \neq 0
\end{aligned} \tag{30}$$

Here

$$\begin{aligned}
\eta_{p,r}^{(H)} &= \frac{\mathcal{N}_1}{(\omega_r - \omega_{\beta_1} + i\gamma_{\beta_1})(\omega_p + \omega_r - \omega_{\alpha_1} - \omega_{\beta_1} + i\gamma_{\alpha_1})} \\
\eta_{q,s}^{(V)} &= \frac{\mathcal{N}_2}{(\omega_s - \omega_{\beta_2} + i\gamma_{\beta_2})(\omega_q + \omega_s - \omega_{\alpha_2} - \omega_{\beta_2} + i\gamma_{\alpha_2})}
\end{aligned} \tag{31}$$

So the joint spectral density is defined as

$$JS_{H-V} = |\eta_{p,r}^{(H)} + e^{i\Delta_{\text{FSS}}\tau_e/\hbar} \eta_{q,s}^{(V)}|^2 \tag{32}$$

With this perspective, we have more degrees of freedom for choosing the relevant parameters

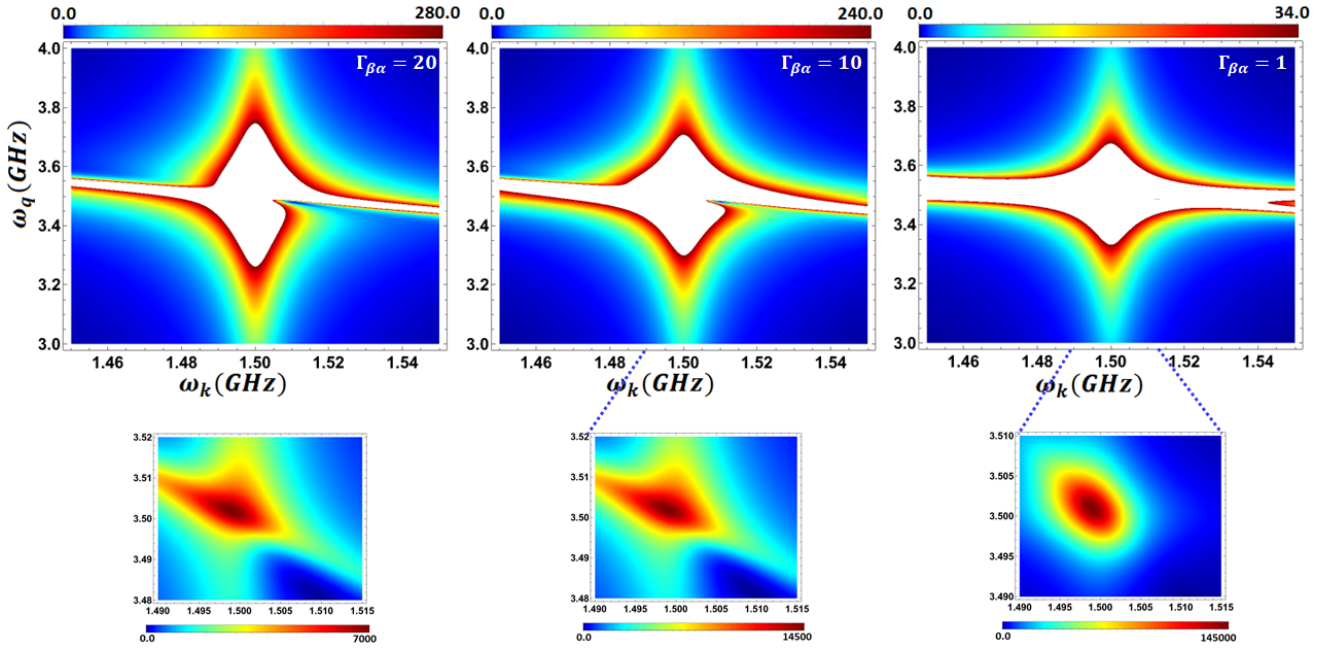


Figure 7: Joint spectral density in cascade emission from typical QD. The polarization of states is included. Different values of  $\Gamma_{\beta\alpha} = \frac{\gamma_{\beta}}{\gamma_{\alpha}}$  and the phase  $\phi = \Delta_{\text{FSS}}\tau_e/\hbar = \pi/4$  are used.

of the system to control purity of the output photons. Studies have shown that the maximum entanglement is obtained when the  $\omega_{\alpha_i} = \omega_{\beta_j}$  and  $\gamma_{\alpha_i} = \gamma_{\beta_j}$  ( where  $i, j = 1, 2$ ).<sup>28,29,63,64</sup> We are mostly interested in predicting the degree of the entanglement by looking at the joint spectral density plotted in Fig. 7. Note that the horizontal axis is relative to the frequency of  $X_{H(V)}$  in the excitonic transitions and the vertical axis is relevant to the frequency of  $XX_{H(V)}$  in the biexcitonic transitions. Compared to the three-level model discussed earlier, here the model is closer to reality and we see more details in the JSD plots. More importantly we see the star shaped emission pattern of exciton and biexciton more explicitly at different frequencies when  $\Gamma_{\beta\alpha}$  is higher. As this ratio becomes smaller from left to right, the probability density becomes more circular in a narrow domain of frequency around  $\omega_{\alpha}$  and  $\omega_{\beta}$  which assures better separation (greater purity) in the photon production. Note that the broken symmetry on the right hand plot can be improved by optimizing geometry of the QD experimentally<sup>37-42</sup> and removing the phase term,  $\phi = \Delta_{\text{FSS}}\tau/\hbar$ . Full analysis and more details of other properties of cascade emitters with this model will be reported in our future work.

## Conclusion

In conclusion, we theoretically studied the underlying mechanism of entangled two-photon generation in semiconductor QD emitters including use of these emitters as an on-demand single photon source. We developed analytical expressions for the characteristic parameters associated with the first- and second- order correlation function, and the Schmidt number of the entangled cascade emission. We extended our model by including for the effects of polarization and fine structure splitting, and the emission delay of the exciton relative to the biexciton. The extended model broadens our vision to see the capacity of other relevant parameters for the practical application of semiconductor quantum dot emitters as single source emitters and offers more details about the underlying mechanism and purity

properties of entangled photon production. Although we have only investigated this effect in the joint spectral density, it is straightforward to include other properties as well. The theoretical studies and the analysis here provides guidelines for the experimental design and engineering of on-demand single photon source applications as diverse as quantum computing and quantum information.

## Supporting Information Available

The following files are available free of charge. The analytical derivations of Schmidt number for cascade emission is explained here.

## Acknowledgement

This work was supported by the U.S. National Science Foundation under Grant No. CHE-1760537. This research was supported in part through the computational resources and staff contributions provided for the Quest high performance computing facility at Northwestern University which is jointly supported by the Office of the Provost, the Office for Research, and Northwestern University Information Technology.

## References

- (1) Utzat, H.; Sun, W.; Kaplan, A. E. K.; Krieg, F.; Ginterseder, M.; Spokoyny, B.; Klein, N. D.; Shulenberger, K. E.; Perkinson, C. F.; Kovalenko, M. V. et al. Coherent single-photon emission from colloidal lead halide perovskite quantum dots. *Science* **2019**, *363*, 1068–1072.
- (2) Cosacchi, M.; Ungar, F.; Cygorek, M.; Vagov, A.; Axt, V. M. Emission-Frequency Separated High Quality Single-Photon Sources Enabled by Phonons. *Phys. Rev. Lett.* **2019**, *123*, 017403.

- (3) Krieg, F.; Ochsenein, S. T.; Yakunin, S.; ten Brinck, S.; Aellen, P.; Süess, A.; Clerc, B.; Guggisberg, D.; Nazarenko, O.; Shynkarenko, Y. et al. Colloidal  $CsPbX_3$  ( $X = Cl, Br, I$ ) Nanocrystals 2.0: Zwitterionic Capping Ligands for Improved Durability and Stability. *ACS Energy Letters* **2018**, *3*, 641–646.
- (4) O’Brien, J. L.; Furusawa, A.; Vučković, J. Photonic quantum technologies. *Nature Photonics* **2009**, *3*, 687.
- (5) Zhang, G.; Haw, J. Y.; Cai, H.; Xu, F.; Assad, S. M.; Fitzsimons, J. F.; Zhou, X.; Zhang, Y.; Yu, S.; Wu, J. et al. An integrated silicon photonic chip platform for continuous-variable quantum key distribution. *Nature Photonics* **2019**, *12*, 839.
- (6) Takeda, S.; Furusawa, A. Toward large-scale fault-tolerant universal photonic quantum computing. *APL Photonics* **2019**, *4*, 060902.
- (7) Kwiat, P. G.; Mattle, K.; Weinfurter, H.; Zeilinger, A.; Sergienko, A. V.; Shih, Y. New High-Intensity Source of Polarization-Entangled Photon Pairs. *Phys. Rev. Lett.* **1995**, *75*, 4337–4341.
- (8) Thompson, J.; Simon, J.; Loh, H.; Vuletic, V. A high-brightness source of narrowband, identical-photon pairs. *Science* **2006**, *313*, 74–77.
- (9) Mosley, P. J.; Lundeen, J. S.; Smith, B. J.; Walmsley, I. A. Conditional preparation of single photons using parametric downconversion: a recipe for purity. *New Journal of Physics* **2008**, *10*, 093011.
- (10) Horn, R.; Abolghasem, P.; Bijlani, B. J.; Kang, D.; Helmy, A. S.; Weihs, G. Monolithic Source of Photon Pairs. *Phys. Rev. Lett.* **2012**, *108*, 153605.
- (11) Heindel, T.; Thoma, A.; von Helversen, M.; Schmidt, M.; Schlehahn, A.; Gschrey, M.; Schnauber, P.; Schulze, J. H.; Strittmatter, A.; Beyer, J. et al. A bright triggered twin-photon source in the solid state. *Nature Communications* **2017**, *8*, 14870.

- (12) Somaschi, N.; Giesz, V.; De Santis, L.; Loredano, M. P., J. C. and Almeida; Hornecker, G.; Portalupi, S. L.; Grange, T.; Antón, C.; Demory, J.; Gómez, C. et al. Near-optimal single-photon sources in the solid state. *Nature Photonics* **2016**, *10*, 340–345.
- (13) Schweickert, L.; Jöns, K. D.; Zeuner, K. D.; Covre da Silva, S. F.; Huang, H.; Lettner, T.; Reindl, M.; Zichi, J.; Trotta, R.; Rastelli, A. et al. On-demand generation of background-free single photons from a solid-state source. *Applied Physics Letters* **2018**, *112*, 093106.
- (14) Ding, X.; He, Y.; Duan, Z.-C.; Gregersen, N.; Chen, M.-C.; Unsleber, S.; Maier, S.; Schneider, C.; Kamp, M.; Höfling, S. et al. On-Demand Single Photons with High Extraction Efficiency and Near-Unity Indistinguishability from a Resonantly Driven Quantum Dot in a Micropillar. *Phys. Rev. Lett.* **2016**, *116*, 020401.
- (15) Schulte, C.; Hansom, J.; Jones, A.; Matthiesen, C.; Le Gall, C.; Atatüre, M. Quadrature squeezed photons from a two-level system. *Nature* **2015**, *525*, 222–225.
- (16) Schlehahn, A.; Thoma, A.; Munnely, P.; Kamp, M.; Höfling, S.; Heindel, T.; Schneider, C.; Reitzenstein, S. An electrically driven cavity-enhanced source of indistinguishable photons with 61% overall efficiency. *APL Photonics* **2016**, *1*, 011301.
- (17) Aharonovich, I.; Englund, D.; Toth, M. Solid-state single-photon emitters. *Nature Photon* **2016**, *10*, 631–641.
- (18) Sapienza, L.; Davanço, M.; Badolato, A.; Srinivasan, K. Nanoscale optical positioning of single quantum dots for bright and pure single-photon emission. *Nature Communications* **2015**, *6*, 7833.
- (19) Gschrey, M.; Gericke, F.; Schüßler, A.; Schmidt, R.; Schulze, J.-H.; Heindel, T.; Rodt, S.; Strittmatter, A.; Reitzenstein, S. In situ electron-beam lithography of deterministic single-quantum-dot mesa-structures using low-temperature cathodoluminescence spectroscopy. *Applied Physics Letters* **2013**, *102*, 251113.

- (20) Senellart, P.; Solomon, G.; White, A. High-performance semiconductor quantum-dot single-photon sources. *Nature Nanotechnology* **2017**, *12*, 1026–1039.
- (21) BROWN, R. H.; TWISS, R. Q. Correlation between Photons in two Coherent Beams of Light. *Nature* **1956**, *177*, 27–29.
- (22) Migdall, A.; Polyakov, S.; Fan, J.; Bienfang, J. *Single-Photon Generation and Detection, Volume 45*; Elsevier, 2013; pp 25–68.
- (23) Hong, C. K.; Ou, Z. Y.; Mandel, L. Measurement of subpicosecond time intervals between two photons by interference. *Phys. Rev. Lett.* **1987**, *59*, 2044–2046.
- (24) Di Martino, G.; Sonnefraud, Y.; Tame, M. S.; Kéna-Cohen, S.; Dieleman, F.; Özdemir, Ş. K.; Kim, M. S.; Maier, S. A. Observation of Quantum Interference in the Plasmonic Hong-Ou-Mandel Effect. *Phys. Rev. Applied* **2014**, *1*, 034004.
- (25) Broome, M. A.; Fedrizzi, A.; Rahimi-Keshari, S.; Dove, J.; Aaronson, S.; Ralph, T. C.; White, A. G. Photonic Boson Sampling in a Tunable Circuit. *Science* **2013**, *339*, 794–798.
- (26) Spagnolo, N.; Vitelli, C.; Bentivegna, M.; Brod, D. J.; Crespi, A.; Flamini, F.; Giacomini, S.; Milani, G.; Ramponi, R.; Mataloni, P. et al. Experimental validation of photonic boson sampling. *Nature Photonics* **2014**, *8*, 615–620.
- (27) Protesescu, L.; Yakunin, S.; Bodnarchuk, M. I.; Krieg, F.; Caputo, R.; Hendon, C. H.; Yang, R. X.; Walsh, A.; Kovalenko, M. V. Nanocrystals of Cesium Lead Halide Perovskites ( $CsPbX_3$ , X = Cl, Br, and I): Novel Optoelectronic Materials Showing Bright Emission with Wide Color Gamut. *Nano Letters* **2015**, *15*, 3692–3696.
- (28) Winik, R.; Cogan, D.; Don, Y.; Schwartz, I.; Gantz, L.; Schmidgall, E. R.; Livneh, N.; Rapaport, R.; Buks, E.; Gershoni, D. On-demand source of maximally entangled photon pairs using the biexciton-exciton radiative cascade. *Phys. Rev. B* **2017**, *95*, 235435.

- (29) Trotta, R.; Wildmann, J. S.; Zallo, E.; Schmidt, O. G.; Rastelli, A. Highly Entangled Photons from Hybrid Piezoelectric-Semiconductor Quantum Dot Devices. *Nano Letters* **2014**, *14*, 3439–3444.
- (30) Keil, R.; Zopf, M.; Chen, Y.; Höfer, B.; Zhang, J.; Schmidt, O. G.; Ding, F.; Schmidt, O. G. Solid-state ensemble of highly entangled photon sources at rubidium atomic transitions. *Nature Communications* **2017**, *8*, 15501.
- (31) Huber, D.; Reindl, M.; Huo, Y.; Huang, H.; Wildmann, J. S.; Schmidt, O. G.; Rastelli, A.; Trotta, R. Highly indistinguishable and strongly entangled photons from symmetric GaAs quantum dots. *Nature Communications* **2017**, *8*, 15506.
- (32) Edamatsu, K. Entangled Photons: Generation, Observation, and Characterization. *Japan Society of Applied Physics* **2007**, *46*, 7175–7187.
- (33) Moradi, T.; Harouni, M. B.; Naderi, M. H. Highly entangled photon pairs generated from the biexciton cascade transition in a quantum-dot–metal-nanoparticle hybrid system. *Phys. Rev. A* **2017**, *96*, 023836.
- (34) Benson, O.; Santori, C.; Pelton, M.; Yamamoto, Y. Regulated and Entangled Photons from a Single Quantum Dot. *Phys. Rev. Lett.* **2000**, *84*, 2513–2516.
- (35) Santori, C.; Fattal, D.; Pelton, M.; Solomon, G. S.; Yamamoto, Y. Polarization-correlated photon pairs from a single quantum dot. *Phys. Rev. B* **2002**, *66*, 045308.
- (36) Stace, T. M.; Milburn, G. J.; Barnes, C. H. W. Entangled two-photon source using biexciton emission of an asymmetric quantum dot in a cavity. *Phys. Rev. B* **2003**, *67*, 085317.
- (37) Stevenson, R. M.; Young, R. J.; Atkinson, P.; Cooper, K.; A., R. D.; Shields, A. J. A semiconductor source of triggered entangled photon pairs. *Nature* **2006**, *439*, 179–182.

- (38) Gerardot, B. D.; Seidl, S.; Dalgarno, P. A.; Warburton, R. J.; Granados, D.; Garcia, J. M.; Kowalik, K.; Krebs, O.; Karrai, K.; Badolato, A. et al. Manipulating exciton fine structure in quantum dots with a lateral electric field. *Applied Physics Letters* **2007**, *90*, 041101.
- (39) Singh, R.; Bester, G. Lower Bound for the Excitonic Fine Structure Splitting in Self-Assembled Quantum Dots. *Phys. Rev. Lett.* **2010**, *104*, 196803.
- (40) Akopian, N.; Lindner, N. H.; Poem, E.; Berlatzky, Y.; Avron, J.; Gershoni, D.; Gerardot, B. D.; Petroff, P. M. Entangled Photon Pairs from Semiconductor Quantum Dots. *Phys. Rev. Lett.* **2006**, *96*, 130501.
- (41) Pathak, P. K.; Hughes, S. Cavity-assisted fast generation of entangled photon pairs through the biexciton-exciton cascade. *Phys. Rev. B* **2009**, *80*, 155325.
- (42) Pathak, P. K.; Hughes, S. Generation of entangled photon pairs from a single quantum dot embedded in a planar photonic-crystal cavity. *Phys. Rev. B* **2009**, *79*, 205416.
- (43) Scully, M.; Zubairy, M. S. *Quantum Optics*; Cambridge University Press, Cambridge, UK, 1997.
- (44) Avanaki, K. N.; Schatz, G. C. Entangled Photon Resonance Energy Transfer in Arbitrary Media. *The Journal of Physical Chemistry Letters* **2019**, *10*, 3181–3188.
- (45) Loudon, R. *The Quantum Theory of Light*; Clarendon Press, Oxford, 1963.
- (46) Morisue, M.; Omagari, S.; Ueno, I.; Nakanishi, T.; Hasegawa, Y.; Yamamoto, S.; Matsui, J.; Sasaki, S.; Hikima, T.; Sakurai, S. Fully Conjugated Porphyrin Glass: Collective Light-Harvesting Antenna for Near-Infrared Fluorescence beyond 1  $\mu\text{m}$ . *ACS Omega* **2018**, *3*, 4466–4474.
- (47) Young, R. J.; Stevenson, R. M.; Atkinson, P.; Cooper, K.; Ritchie, D. A.; Shields, A. J.

- Improved fidelity of triggered entangled photons from single quantum dots. *New Journal of Physics* **2006**, *8*, 29.
- (48) Coles, D. M.; Somaschi, N.; Michetti, P.; Clark, C.; Lagoudakis, P. G.; Savvidis, P. G.; Lidzey, D. G.; and, Polariton-mediated energy transfer between organic dyes in a strongly coupled optical microcavity. *Nature Materials* **2014**, *13*, 712.
- (49) Zhong, X.; Chervy, T.; Wang, S.; George, J.; Thomas, A.; Hutchison, J. A.; Devaux, E.; Genet, C.; Ebbesen, T. W. Non-Radiative Energy Transfer Mediated by Hybrid Light-Matter States. *Angewandte Chemie International Edition* **2016**, *55*, 6202–6206.
- (50) Zhong, X.; Chervy, T.; Zhang, L.; Thomas, A.; George, J.; Genet, C.; Hutchison, J. A.; Ebbesen, T. W. Energy Transfer between Spatially Separated Entangled Molecules. *Angewandte Chemie International Edition* **2017**, *56*, 9034–9038.
- (51) Ripka, F.; Kübler, H.; Löw, R.; Pfau, T. A room-temperature single-photon source based on strongly interacting Rydberg atoms. *Science* **2018**, *362*, 446–449.
- (52) Crocker, C.; Lichtman, M.; Sosnova, K.; Carter, A.; Scarano, S.; Monroe, C. High purity single photons entangled with an atomic qubit. *Opt. Express* **2019**, *27*, 28143–28149.
- (53) Silva, B.; Sánchez Muñoz, C.; Ballarini, D.; González-Tudela, A.; de Giorgi, M.; Gigli, G.; West, K.; Pfeiffer, L.; del Valle, E.; Sanvitto, D. et al. The colored Hanbury Brown–Twiss effect. *Scientific Reports* **2016**, *6*, 37980.
- (54) Kiraz, A.; Atatüre, M.; Imamoglu, A. Quantum-dot single-photon sources: Prospects for applications in linear optics quantum-information processing. *Phys. Rev. A* **2004**, *69*, 032305.
- (55) Ahn, K. J. Temporal dynamics of zero-delay second order correlation function and spectral entanglement of two photons emitted from ladder-type atomic three-level systems. *Opt. Express* **2020**, *28*, 1790–1804.

- (56) Hamsen, C.; Tolazzi, K. N.; Wilk, T.; Rempe, G. Strong coupling between photons of two light fields mediated by one atom. *Nature Physics* **2018**, *14*, 885–889.
- (57) He, Y.-M.; Iff, O.; Lundt, N.; Baumann, V.; Davanco, M.; Srinivasan, K.; Höfling, S.; Schneider, C. Cascaded emission of single photons from the biexciton in monolayered  $WSe_2$ . *Nature Communications* **2016**, *7*, 13409.
- (58) Law, C. K.; Walmsley, I. A.; Eberly, J. H. Continuous Frequency Entanglement: Effective Finite Hilbert Space and Entropy Control. *Phys. Rev. Lett.* **2000**, *84*, 5304–5307.
- (59) Eberly, J. H. Schmidt analysis of pure-state entanglement. *Laser Physics* **2006**, *16*, 921–926.
- (60) Chen, C.; Bo, C.; Niu, M. Y.; Xu, F.; Zhang, Z.; Shapiro, J. H.; Wong, F. N. C. Efficient generation and characterization of spectrally factorable biphotons. *Opt. Express* **2017**, *25*, 7300–7312.
- (61) Lamata, L.; León, J. Dealing with entanglement of continuous variables: Schmidt decomposition with discrete sets of orthogonal functions. *Journal of Optics B: Quantum and Semiclassical Optics* **2005**, *7*, 224–229.
- (62) Valencia, A.; Ceré, A.; Shi, X.; Molina-Terriza, G.; Torres, J. P. Shaping the Waveform of Entangled Photons. *Phys. Rev. Lett.* **2007**, *99*, 243601.
- (63) Hudson, A. J.; Stevenson, R. M.; Bennett, A. J.; Young, R. J.; Nicoll, C. A.; Atkinson, P.; Cooper, K.; Ritchie, D. A.; Shields, A. J. Coherence of an Entangled Exciton-Photon State. *Phys. Rev. Lett.* **2007**, *99*, 266802.
- (64) Stevenson, R. M.; Hudson, A. J.; Bennett, A. J.; Young, R. J.; Nicoll, C. A.; Ritchie, D. A.; Shields, A. J. Evolution of Entanglement Between Distinguishable Light States. *Phys. Rev. Lett.* **2008**, *101*, 170501.